Geophys. J. R. astr. Soc. (1973) **35**, 265–276.

Finite Amplitude Convection Through a Phase Boundary

Frank M. Richter

(Received 1972 November 25)

Summary

A finite amplitude, numerical model of convective motions through a phase boundary is studied. The phase change is assumed to occur over a finite vertical transition zone in the fluid and thus a continuously stratified model is considered. The motions are driven by horizontal temperature gradients on the boundaries or super-critical vertical stratification. In the case of Rayleigh instability, the numerical results reproduce the neutral curve previously obtained in the analytic solution of the linearized problem. When the parameters of the problem are chosen to simulate the olivine–spinel transition in the upper mantle, the following results are obtained: (1) the vertical scale of motion is the entire depth of the fluid; (2) the horizontal scale is not significantly changed from the case of a single phase fluid; (3) the amplitude of the motion is not significantly changed, due to buoyancy changes at the phase boundary being offset by corresponding sources and sinks of latent heat; and (4) the phase boundary varies in depth by as much as 30 km when the vertical velocities are of the order of 10^{-1} cm yr^{-1}.

Introduction

The concept of plate tectonics (Isacks, Oliver & Sykes 1968) implies a mass transport in the upper mantle which balances the mass flux of moving lithospheric plates. The nature of this return flow is not determined by surface geophysical observations and present understanding relies on fluid dynamic models. In order to formulate realistic models it is important to identify those properties of the upper mantle which have significant effect on mass transports within it. This study isolates a single property, mineralogical phase changes, and investigates their effect on the dynamics of finite-amplitude motions.

The importance of mineralogical phase changes was recognized by Birch (1952) and recent work (Anderson 1970) relates seismic ‘ discontinuities ’ to specific phase transitions in the upper mantle. In a dynamic sense, these phase changes will act as local sources of buoyancy and heat and thus influence motions which penetrate the boundary between phases. The mathematical study of the dynamic role of a univariant phase transition was begun by Busse & Schubert (1971) by considering a linearized model problem which determines the stability of a stratified two-phase system. The results of the linear problem were applied to the mantle by Schubert & Turcotte (1971), who also discuss prior thinking regarding the role of phase changes.

The principal result of the linear theory is summarized by the stability diagram for Rayleigh–Benard convection through a phase boundary shown in Fig. 1 taken from the article by Schubert & Turcotte (1971). The family of curves map the critical Rayleigh number, above which the two-phase system is unstable, as a function of the properties of the phase change. The non-dimensional parameters are defined:

$$R_a = \frac{g\alpha\Delta T D^3}{K\nu},$$

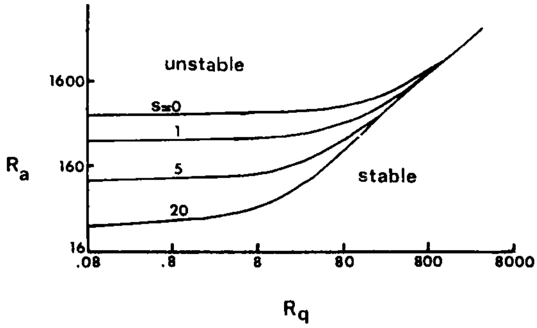

FIG. 1. Stability fields for Rayleigh–Benard convection through a phase boundary after Schubert & Turcotte (1971).

Rayleigh number based on vertical temperature scale ΔT;

$$R_Q = \frac{g\alpha q_L D^3}{C_p K\nu},$$

Rayleigh number based on energy released by material changing phase;

$$S = \frac{2\Delta\rho}{\rho\alpha D(\rho g/\gamma - \beta)},$$

a measure of the density change across the phase boundary;

where **g** is the acceleration of gravity, α the coefficient of thermal expansion, K the thermometric conductivity, ν the kinematic viscosity, ρ the density, D the total depth of the two-phase system, q_L the energy released per unit mass of material changing phase, β the vertical temperature gradient in the undisturbed state, C_p the specific heat at constant pressure, and γ is the slope of the Clapeyron curve. The Clapeyron curve describes the locus of pressure–temperature points at which phase transition occurs in a univariant system in thermodynamic equilibrium. The slope γ is related to other parameters of the problem by:

$$\gamma = \frac{q_L \rho_1 \rho_2}{T\Delta\rho}.$$

The effect of a given phase change on the stability of the entire system is determined by comparing the critical Rayleigh number for the two-phase system to the point $S = 0$, $R_Q = 0$, which is the critical Rayleigh number for the equivalent single-phase system (R_c). The phase boundary will appear a barrier to convection only if the critical Rayleigh number for the two-phase system is greater than the Rayleigh number required for either phase to convect separately. It must be recognized that the Rayleigh number (based on D) for a phase of depth extent d ($d < D$) to convect must be greater than $(D/d)^4 R_c$.

The linear theory, by assumption, is valid only for infinitesimal amplitudes. A logical extension is to consider the non-linear problem and thus extend the validity of the analysis into the finite amplitude regime. The non-linear theory presented in this study will determine the effect of a univariant phase change on the amplitude of motions through the phase boundary and the effect of a finite amplitude motion field on the local depth to the phase boundary.

Model and governing equations

I will consider the idealized fluid dynamic problem of motions through a univariant phase change in a horizontal layer of very viscous fluid. The fluid motions can be forced by an imposed horizontal temperature variation $\tau(x)$ or result from a supercritical vertical temperature gradient controlled by ΔT. The two-dimensional model is shown in Fig. 2. Each phase is assumed Newtonian, Boussinesq, non-rotating, incompressible and non-dissipative. The coefficient of expansion α, the kinematic viscosity ν, and the thermometric diffusivity K are assumed uniform throughout the entire system.

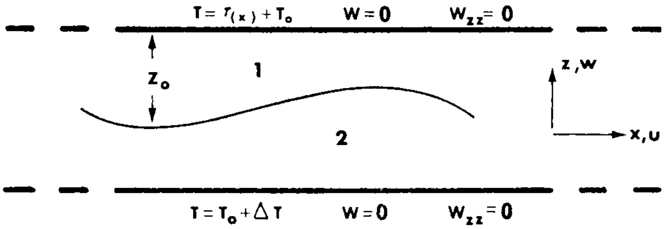

FIG. 2. Model for convection in a two-phase fluid.

The temperature is non-dimensionalized using the temperature scale ΔT.

$$\theta = (T-T_0)/\Delta T \tag{1}$$

The density is then written:

$$\rho = \rho_1(1-\alpha\Delta T\theta+\Delta\rho\Gamma) \tag{2}$$

where

$$\Delta\rho = (\rho_2-\rho_1)/\rho_1. \tag{3}$$

The subscripts refer to the phase and Γ, a function of x and z, is the fractional concentration of phase 2. The equation of state (2) is valid throughout the entire fluid and includes the effects of thermal expansion and phase change but ignores the effect of pressure on the density. The neglect of any direct pressure dependence is consistent with the assumptions and further can be shown to have no significant dynamic consequence.

If $\alpha \ll 1$ and $\Delta\rho \ll 1$, the Boussinesq approximation (see, Spiegel & Veronis 1960) allows density variations to be ignored in all terms of the momentum equation except where multiplied by gravity (buoyancy terms). Under this approximation the dimensionless momentum equation is:

$$D\vec{q}/Dt = -\nabla p+\frac{g\alpha\Delta TD^3\theta\hat{k}}{K^2}-\frac{\Delta\rho gD^3}{K^2}\Gamma\hat{k}+(\nu/K)\nabla^2\vec{q} \tag{4}$$

where distances are non-dimensionalized using the total depth D, the velocity vector $\vec{q}$ using K/D, time using D^2/K, and pressure using $\rho K^2/D^2$. The operators are:

$$D/Dt = \partial/\partial t+\vec{q}\cdot\nabla$$

$$\nabla = \hat{\imath}\,\partial/\partial x+\hat{k}\,\partial/\partial z$$

$$\nabla^2 = \partial^2/\partial x^2+\partial^2/\partial z^2$$

$\hat{\imath}$ and $\hat{k}$ are unit vectors in x and z respectively.

Equation (4) is transformed into an equation governing the vorticity η (defined as $\nabla\times\vec{q}$) by taking $\nabla\times$ the momentum equation

$$\partial\eta/\partial t = J(\psi,\eta)-\sigma R_a\,\partial\theta/\partial x+\sigma R_p\,\partial\Gamma/\partial x+\sigma\nabla^2\eta \tag{5}$$

where

$$R_a = \frac{g\alpha\Delta TD^3}{K\nu},\quad R_p = \frac{g\Delta\rho D^3}{K\nu},\quad \sigma = \nu/K,$$

ψ is the stream function and $J(\, , \,)$ is the Jacobian operator $\partial(\, , \,)/\partial(x, z)$. In the limit of large Prandtl number σ, equation (5) can be approximated by:

$$\nabla^2\eta = R_a \, \partial\theta/\partial x - R_p \, \partial\Gamma/\partial x. \tag{6}$$

The neglected terms are order $1/\sigma$ which is approximately 10^{-24} in the mantle.

The stream function is related to the vorticity by:

$$\nabla^2\psi = \eta. \tag{7}$$

The velocity field can be obtained from the stream function by the relations:

$$u = \partial\psi/\partial z, \quad w = -\partial\psi/\partial x. \tag{8}$$

In steady state the streamlines map the trajectories of fluid parcels.

The temperature equation appropriate to a two-phase system must take into account the energy absorbed or released by material changing phase. The rate of energy exchange is written:

$$Q_L = \rho q_L \, D\Gamma/Dt \quad (\mathrm{cal\,cm^{-3}\,s^{-1}}) \tag{9}$$

where q_L is the energy released per unit mass of material changing from phase 1 to phase 2. Including Q_L as a heat source (or sink) the temperature equation is:

$$DT/Dt = K\nabla^2 T + Q_L/\rho C_p \tag{10}$$

Non-dimensionalizing as in the momentum equation (4), equation (10) can be written in terms of the stream function and the definition of Q_L.

$$\partial\theta/\partial t = J[\psi, \theta - (R_Q/R_a)\,\Gamma] + (R_Q/R_a)\,\partial\Gamma/\partial t + \nabla^2\theta \tag{11}$$

where

$$R_Q = \frac{g\alpha(q_L/C_p)\,D^3}{K\nu}.$$

Up to this point we have three equations, (6), (7) and (11) for four unknowns, η, θ, ψ and Γ. The final relation required to close the system is provided by the Clapeyron relation which specifies the phase boundary in pressure–temperature co-ordinates. If the dimensional temperature field $T(x, z)$ is known, a function $Z_0(x)$ can be found such that $T[x, Z_0(x)]$ is always on the Clapeyron curve. $Z_0(x)$ is interpreted to represent the depth to the phase boundary as defined by the surface $\Gamma = 0{\cdot}5$ (50 per cent concentration of each phase). The vertical structure of Γ is formally arbitrary but is specified so as to provide a transition region of finite thickness. The exact vertical structure of Γ is not very important to the problem at hand, which can be seen by considering equation (6). The term $R_p \, \partial\Gamma/\partial x$ is a source term in a Poisson equation and thus one expects that as long as the transition region is small compared to the total depth of the fluid, the total change in Γ is the important quantity rather than the details of its vertical structure.

The boundary conditions are shown in Fig. 2. The temperature boundary condition contains a horizontal variation $\tau(x)$ and a vertical temperature change ΔT. The dynamic boundary conditions are no vertical velocity at horizontal boundaries ($w = 0$) and no stress ($u_z = 0$ or $w_{zz} = 0$). The no stress boundary condition replaces the no slip condition ($u = 0$) in order that results may be compared to the analytic results of the prior linear theory.

The governing equations are solved numerically. The temperature equation is written in finite difference form using the scheme proposed by Dufort & Frankel (1953). The finite difference analogue to equation (11) is:

$$\begin{aligned}\frac{\theta_{i,j}^{n+1} - \theta_{i,j}^{n-1}}{2\Delta t} &= J_A(\psi^n, \theta^n - (R_Q/R_a)\,\Gamma^n) + (R_Q/R_a)\,\frac{(\Gamma_{i,j}^{n} - \Gamma_{i,j}^{n-1})}{\Delta t} \\ &\quad + (1/\Delta x)^2\,(\theta_{i+1,j}^{n} + \theta_{i-1,j}^{n} - \theta_{i,j}^{n+1} - \theta_{i,j}^{n-1}) \\ &\quad + (1/\Delta z)^2\,(\theta_{i,j+1}^{n} + \theta_{i,j-1}^{n} - \theta_{i,j}^{n+1} - \theta_{i,j}^{n-1})\end{aligned} \tag{12}$$

where N measures the time step, i and j are the x and z grid points respectively, and $J_A(\alpha, \beta)$ is the Jacobian operator using the Arakawa formulation (Arakawa 1966) which conserves α, α^2, β and β^2.

In order to find θ^{n+1} we need Γ^n. The phase boundary is assumed to be the $\Gamma = 0{\cdot}5$ surface. The depth to the phase boundary, $Z_{0i}{}^n$ is found by determining the intersection at each i of the temperature–depth profile $[\theta^n(j)]$ with the Clapeyron curve written in temperature–depth co-ordinates. The intersection can be found by any standard technique. Having found $Z_{0i}{}^n$, $\Gamma_{i,j}{}^n$ is written:

$$\Gamma_{i,j}{}^n = \tfrac{1}{2}(1+\tanh([Z_{0i}{}^n - j(\Delta z)]\, L)). \tag{13}$$

The vertical structure of Γ is assumed to be a hyperbolic tangent centred at Z_{0i} and varying on a length scale L. If $L \ll D$ the arbitrariness of the choice of Γ's vertical structure will not affect the solutions θ and η. Having $\Gamma_{i,j}{}^n$, $\theta_{i,j}{}^{n+1}$ is found from equation (12).

In solving equation (12), the advective stability criterion requires that the time step ΔT be limited such that

$$(U_m\, \Delta t)/\delta < 1$$

where U_m is the maximum velocity and δ is the grid spacing. Even though the Dufort–Frankel scheme does not require it, it was found best to also satisfy a diffusive stability condition

$$\Delta t < \delta^2.$$

Once the temperature field is updated, Γ is updated and the 'source' terms in the vorticity equation (6) determined. The no-stress boundary condition ($w_{zz} = 0$) is equivalent to zero vorticity on the boundaries. Equation (6) is a Poisson equation which is solved very efficiently using the non-iterative scheme developed by Buneman (1969). Having the updated vorticity field, the stream function is found by solving (7) using the same method. The boundary conditions in terms of the stream function are that it be zero on horizontal boundaries.

The numerical calculation is performed over a finite domain and thus boundary conditions must be specified on two vertical boundaries. I impose the condition that all fields be periodic about the two ends of the fluid layer. This condition simulates an annulus in which sphericity has been ignored.

Solutions

Two classes of flows were considered: (1) horizontal convection driven primarily by temperature variations on the boundaries, and (2) Rayleigh–Benard convection. Horizontal convection is the more useful of the two in estimating the effect of the phase change on the structure of the resulting flow. Horizontal convection has more freedom in its horizontal structure than Rayleigh–Benard convection which is limited to a discrete wavenumber spectrum by the finite horizontal dimension of the domain of calculation. The Rayleigh–Benard model on the other hand has the important advantage that it will provide an estimate of numerical accuracy when compared to analytical results.

Horizontal convection

Fig. 3 is typical of horizontal convection through a phase boundary. The non-dimensional temperature and stream function fields are shown as well as the dimensional change in elevation of the $\Gamma = 0{\cdot}5$ surface (when the depth is dimensionalized using $D = 1000$ km). The temperature boundary conditions are $\theta = 1$ at $z = 0$ and θ ranging from 0 to 0·2 at $z = 1$ as indicated by the intersection of the isotherms with the boundary. The dynamic boundary conditions are $\psi = 0$ and $\eta = 0$ ('free') at $z = 0$ and $z = 1$. Periodic boundary conditions are imposed at $x = 0$ and $x = 25$ which are satisfied by considering the temperature to be symmetric and the stream function antisymmetric around $x = 12{\cdot}5$. The concentration function $\Gamma(x, z)$ is such that the transition from one phase to another occurs over a depth of $0{\cdot}1\ D$. The constant T_0 is also specified because together with ΔT it determines the mean depth of the phase boundary. In the case shown in Fig. 3, T_0 is 1200 °C and the remaining

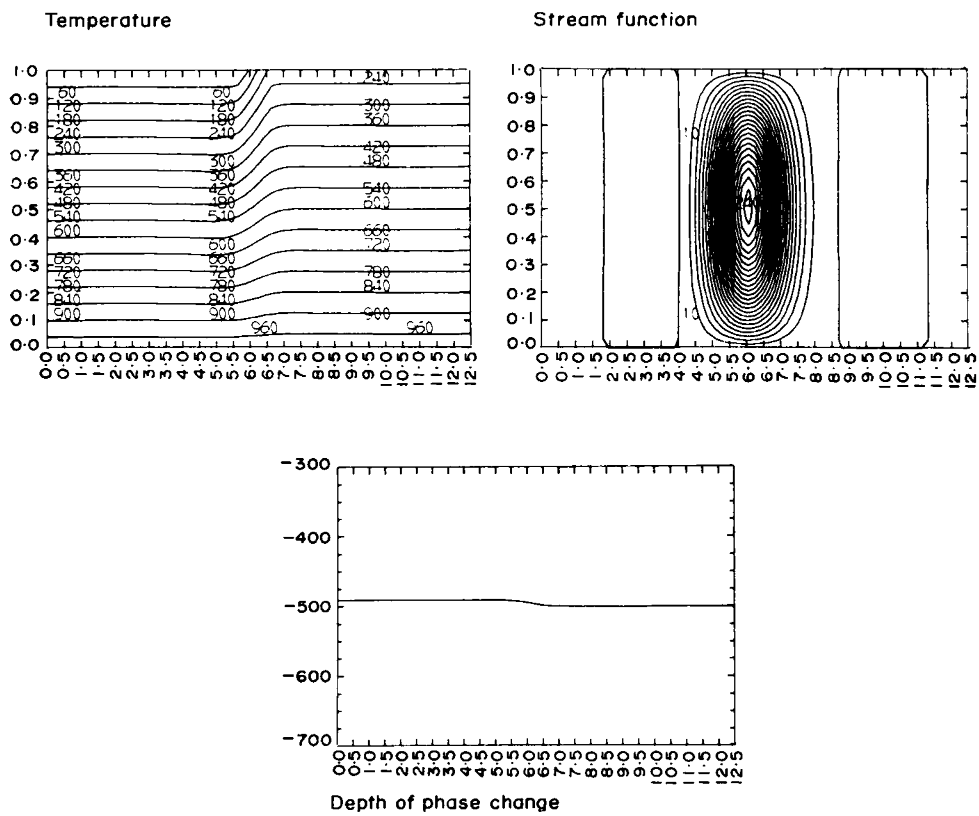

FIG. 3. Non-dimensional temperature and stream function, and dimensional depth to phase boundary when $R_a = 100$, $R_p = 1600$, $R_Q = 24$, $\Delta T = 500$ °C, $T_0 = 1200$ °C and $D = 1000$ km. Stream function contours from 0 to 0·24, temperature contours from 0 to 1·0.

parameters R_a, R_p and R_Q have values of 100, 1600 and 24, respectively. The slope of the Clapeyron curve ($\gamma = q_L \rho_1 \rho_2 / \Delta\rho T$) is determined once R_Q and R_p are specified. A slope of 6 °C km^{-1} is consistent with the above values of R_Q and R_p. This slope, which is considered constant, is approximately the estimated value for the Forsterite–Spinel transition (Anderson 1970).

In order to get an idea of the effect of the phase change in this parameter range, we can compare Fig. 3 to Fig. 4 which is the same calculation with R_p and R_Q set to zero. The phase change increases the amplitude by a factor of three but the structure of the solution is unchanged. The increased amplitude when the phase change is present is not surprising. The family of neutral curves in Fig. 1 suggest that the case $R_Q = 24$, $R_p = 1600$ ($S = 2$) is more unstable than $R_Q = 0$, $R_p = 0$. The depth to the phase boundary as measured by the $\Gamma = 0{\cdot}5$ surface is greater in warmer regions of the fluid which one would expect for all cases with positive Clapeyron slope.

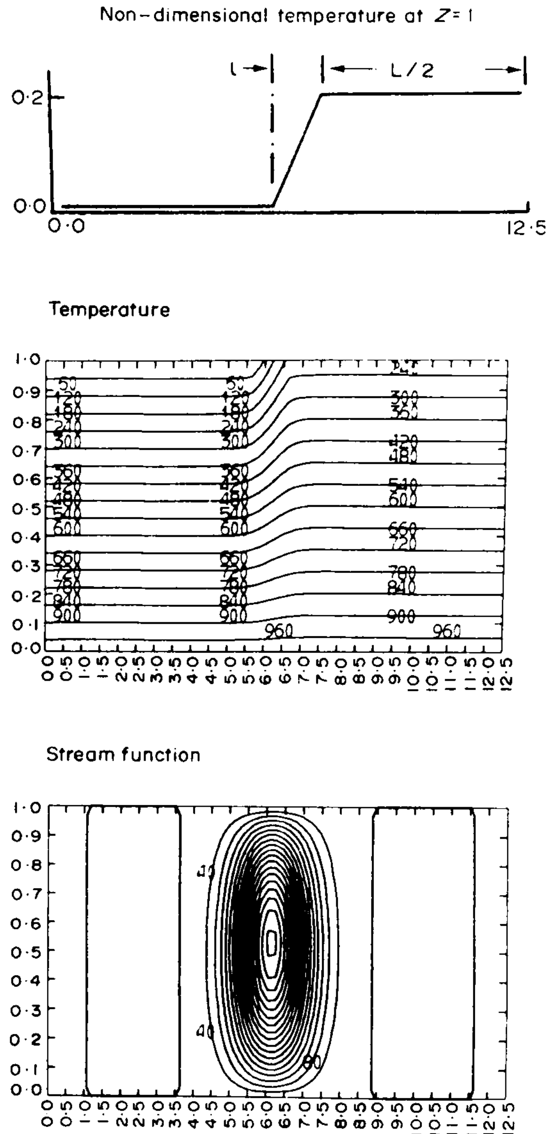

FIG. 4. Same case as Fig. 3 except that phase change is suppressed by setting $R_P = 0$, $R_Q = 0$. Stream function contours from 0 to 0·072, temperature contours from 0 to 1·0.

Rayleigh–Benard convection

Two groups of numerical experiments were considered. The first group was designed to determine the critical Rayleigh number for Rayleigh–Benard convection through a phase boundary. The numerically determined critical Rayleigh number can then be compared to the appropriate point on the family of neutral curves in Fig. 1. The second group of experiments explore the finite amplitude regime.

The critical Rayleigh number for the two-phase system was estimated by varying the Rayleigh number until two values sufficiently close together were found such that perturbations grew for one value and decayed for the other. The growth or decay of the perturbations was determined by observing the temperature and vorticity field over long periods of time. Such a method of estimating the critical Rayleigh number is very costly in terms of computer time due to the small growth or decay rates near the neutral curve. For this reason, only three cases were considered:

(1) $R_Q = 0$, $S = 2$,
(2) $R_Q = 240$, $S = 0$,
(3) $R_Q = 100$, $S = 2$.

In all three cases, the phase change occurs at a mean depth of $D/2$ (specified by T_0) and the boundaries are ' free ' in order that the numerical model reproduce the same problem considered in the linear theory.

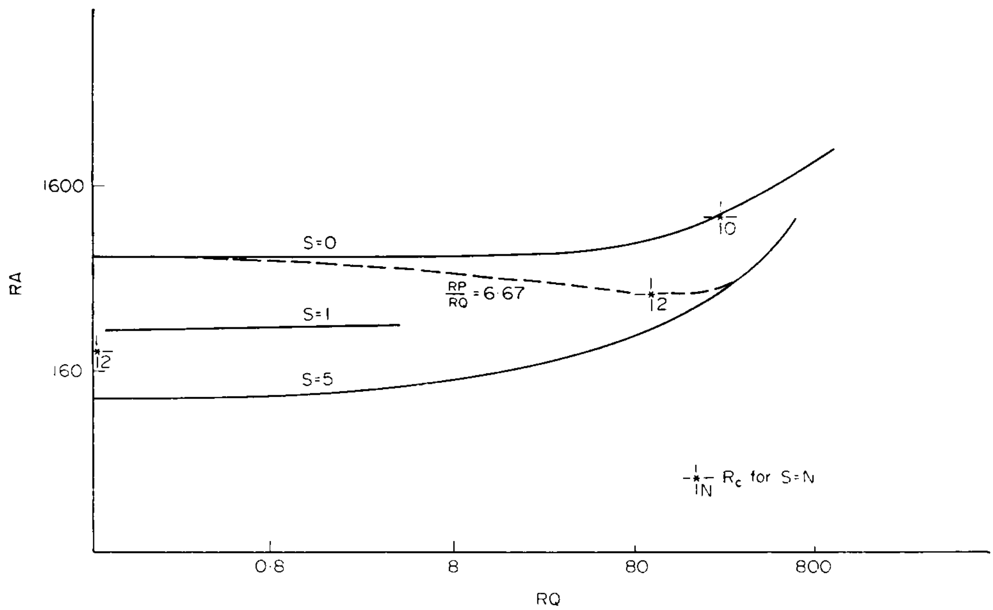

FIG. 5. Numerically determined critical Rayleigh numbers and analytical neutral curves.

The numerical critical Rayleigh numbers can be compared to their analytically predicted value by plotting them on a graph of the relevant analytical neutral curves as shown in Fig. 5. The dashed curve shows the critical Rayleigh number versus R_Q for constant Clapeyron slope of $6\,^{\circ}\mathrm{C\,km^{-1}}$. The excellent agreement between the numerical results and the linear theory can be taken as a measure of the accuracy of the numerical techniques used. The choice of a finite phase transition zone of thickness $0{\cdot}1D$, instead of a discontinuity as assumed in the linear theory, has no observable effect on the stability of the fluid.

We now consider the finite amplitude regime. Fig. 6 shows a typical case of steady Rayleigh–Benard convection through a phase boundary. The boundary conditions are:

$$\theta = 0, \quad \eta = \psi = 0, \quad z = 1,$$
$$\theta = 1, \quad \eta = \psi = 0, \quad z = 0.$$

Periodic boundary conditions are imposed at $x = 0$ and $x = 25$, which are satisfied if the temperature field is symmetric and the stream function antisymmetric about $x = 12{\cdot}5$. The non-dimensional parameters are: $R_a = 500$, $R_p = 8000$, and $R_Q = 120$, and this choice implies a Clapeyron slope of $6\,^{\circ}\mathrm{C\,km^{-1}}$. These parameters

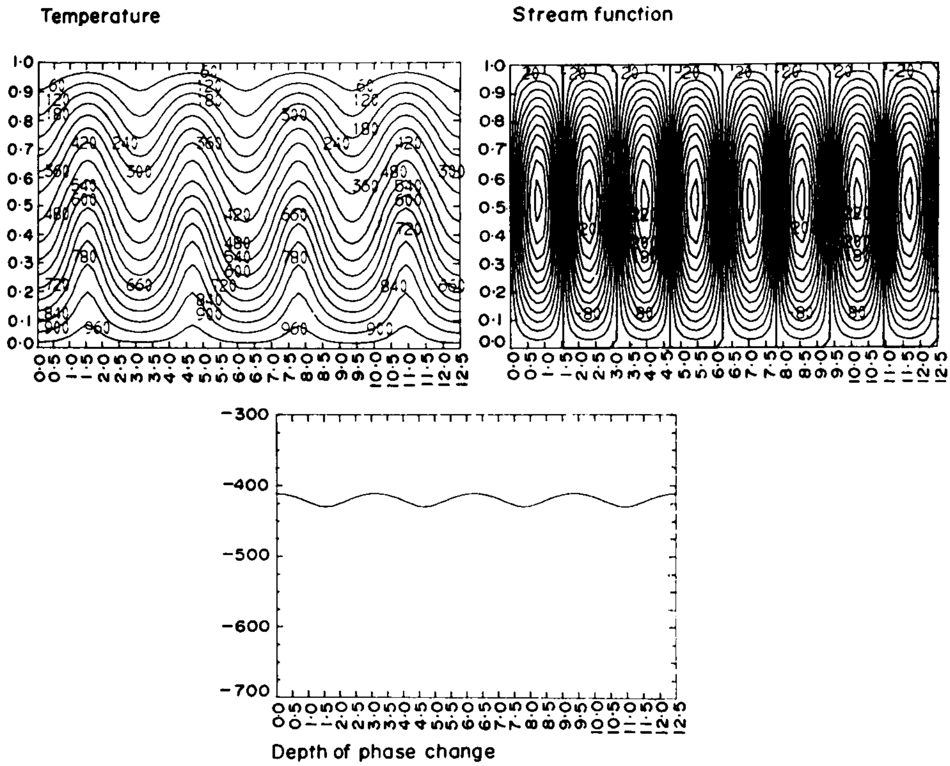

FIG. 6. Steady Rayleigh–Benard convection through a phase boundary having the properties of the Olivine–Spinel transition. $R_a = 500$, $R_D = 8000$, $R_Q = 120$, $\Delta T = 500\,°C$, $T_0 = 1200\,°C$, and $D = 1000$ km. Non-dimensional stream function contours from $-2{\cdot}2$ to $2{\cdot}2$, non-dimensional temperature contours from 0 to 1·0.

will result from a vertical temperature change of 500 °C, $\Delta\rho = 0{\cdot}08$ and $q_L = 40$ cal g^{-1} when $g\alpha D^3/K\nu$ is one. These values for $\Delta\rho$ and q_L are those considered by Schubert & Turcotte (1971) to be typical of the Olivine–Spinel transition in the upper mantle. The effect of the phase change is clearly destabilizing since $R_a = 500$ is subcritical in the absence of a phase change. The phase boundary ($\Gamma = 0{\cdot}5$ surface) has periodic changes in elevation which result from the horizontal variations of the temperature field. The phase boundary is at shallower depth in regions of downwelling since the downwelling promotes locally cooler temperatures.

It is interesting to compare the amplitude of Rayleigh–Benard convection through a phase boundary to the amplitude of single-phase convection. Fig. 7 shows the steady state amplitude of both cases as a function of the Rayleigh number. The parameter range was chosen to include a phase change having the properties of the Olivine–Spinel transition in the upper mantle. The effect of the phase change is to increase the amplitude of Rayleigh–Benard convection for all values of R_a.

The amplitude of steady Rayleigh–Benard convection in a single-phase system can be written in terms of the Rayleigh number as:

$$A = C_1\left(\frac{R_a - R_c}{R_c}\right)^{1/2}$$

where

$$R_c = \text{critical Rayleigh number} = 657{\cdot}5$$

$$C_1 = \text{constant} = 10{\cdot}88.$$

The amplitude data for convection through a phase boundary can be fitted by a similar relation if $C_1 = 23$ and $R_c = 450$. This suggests that for Rayleigh numbers greater than 1000 the effect of the phase change will be to increase the amplitude by a factor of approximately two.

Fig. 7 also shows the effect of finite amplitude convection on the elevation of the phase boundary for the same three cases shown in the upper graph. By using the graphs, vertical velocities can be related to changes in phase boundary elevation. If the velocity is dimensionalized using $D = 1000$ km and $K = 10^{-2}\,\mathrm{cm^2\,s^{-1}}$, then a vertical velocity of 0·1 $\mathrm{cm\,yr^{-1}}$ results in approximately a 15-km change in the phase boundary elevation from its mean value (peak to peak change of 30 km).

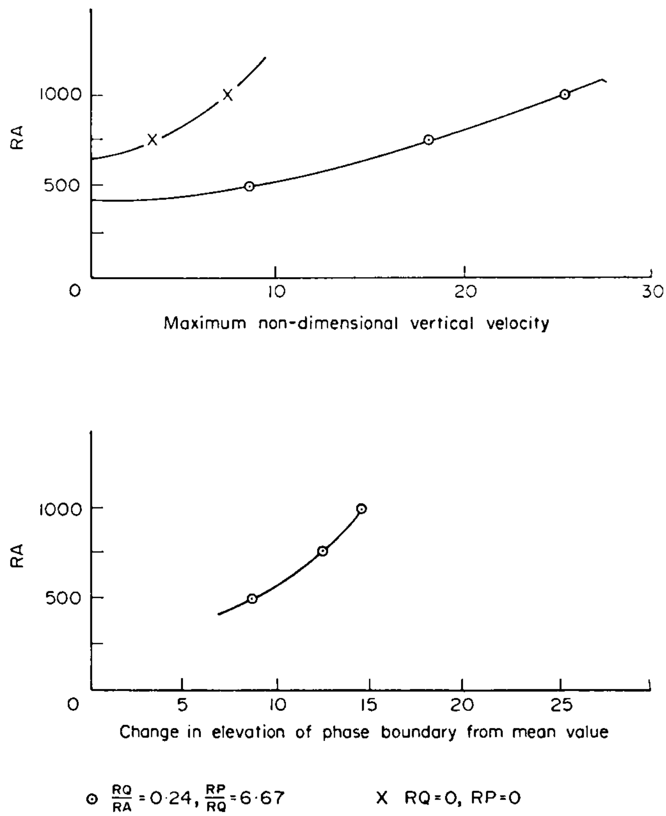

FIG. 7. Effect of phase change on the amplitude of Rayleigh–Benard convection and change in phase boundary depth due to convection. Depth dimensionalized using $D = 1000$ km.

Up to this point, we have restricted our attention to phase changes with positive Clapeyron slopes. Ahrens & Syono (1967) suggest that the transformation of Mg_2SiO_4 in the spinel structure to periclase and SiO_2 in the stishovite structure, which occurs at an average depth of 800 km, has a negative Clapeyron slope. A numerical calculation was performed using their parameters for this reaction in the hope that a phase change with negative slope would prove a barrier to vertical motions and thus provide a determinable lower boundary to the asthenosphere. The calculations showed that a phase change having the properties of the Spinel–Stishovite transition is mildly stabilizing (compared to no phase change) but it is not a barrier to vertical motions. The principal effect of the negative slope of the Clapeyron curve is that now the phase boundary is at shallower depth in regions of upwelling.

It is at first surprising to find that changing the slope of the Clapeyron curve from positive to negative has so little effect on flows through the phase boundary. This lack of dramatic effect can best be understood by considering the equations governing the system. The vorticity equation is:

$$\nabla^2 \eta = R_a\, \partial T/\partial x - R_p\, \partial \Gamma/\partial x.$$

If the Clapeyron curve has positive slope, then $\partial T/\partial x$ and $\partial \Gamma/\partial x$ have everywhere opposite sign as can be seen in Fig. 6. Therefore, both these sources generate vorticity of the same sign. This implies that the term $R_p\, \partial \Gamma/\partial x$ is destabilizing. On the other hand, cellular motions will cause heat to be released in regions of downwelling and absorbed in regions of upwelling. This has the effect of decreasing horizontal temperature gradients and thus degrades a source of vorticity. If the Clapeyron curve has negative slope, a similar line of reasoning leads one to conclude that the term $R_p\, \partial \Gamma/\partial x$ is now a sink for vorticity generated by $\partial T/\partial x$, while the energy of phase change enhances the source $\partial T/\partial x$. The difference between the positive and negative Clapeyron slope cases is that the role of the two opposing dynamical properties of the phase change are reversed.

Conclusions

One of the motivating factors in seeking to understand the dynamic role of mineralogical phase changes was to determine if their effect was sufficiently great to warrant their inclusion in present dynamic models of the upper mantle. The principal dynamic effects found were:

(1) Phase changes may change the critical Rayleigh number for the onset of Rayleigh–Benard convection (already known from prior linear theory).

(2) Phase changes may change the steady amplitude of motions through a phase boundary by a numerical factor.

(3) The structure of the motion field is not significantly changed by the presence of the phase change.

In estimating the importance of these effects one must keep in mind the uncertainties which exist regarding other dynamically important quantities in the upper mantle. For example, the dynamically significant quantity for Rayleigh–Benard convection is the difference between the actual and the critical Rayleigh number. If the actual Rayleigh number is not known to within an order of magnitude, then the neglect of the shift in critical Rayleigh number due to phase changes is of little importance. A similar argument can be made in connection with forced flows by comparing the change in amplitude due to phase changes to present uncertainty of the magnitude of the forcing and other mantle parameters which affect the amplitude. It appears that phase changes provide a correction term to the system's amplitude which is small compared to present capability to predict that amplitude.

In hindsight, the more important consideration is the effect of the motion field on the depth to the phase boundary. Since there is little hope of directly measuring velocities in the upper mantle, it is important to establish the relationship between mass transport and some measurable property of the mantle. If changes in phase boundary elevation of the order of tens of kilometres are measurable by geophysical observations, then the techniques used in this study provide an indirect method of estimating the velocity field in the upper mantle.

Acknowledgments

This work was supported under NSF grants GA-11951 and GA-28427 while the author was at the University of Chicago. Acknowledgment is made to the National

Center for Atmospheric Research, which is sponsored by the National Science Foundation, for computer time used in this research.

Department of Earth and Planetary Science,
Massachusetts Institute of Technology,
Cambridge, Massachusetts 02139

References

Ahrens, T. J. & Syono, Y., 1967. Calculated mineral reactions in the Earth's mantle, *J. geophys. Res.*, **72,** 4181.

Anderson, D. L., 1970. Petrology of the mantle, *Mineral. Soc. Amer. Spec. Pap.*, **3,** 85.

Arakawa, A., 1966. Computational design of long-term numerical integration of equations of fluid motions: two-dimensional incompressible flow, part 1, *J. Computational Physics*, **1,** 119.

Birch, F., 1952. Elasticity and constitution of the Earth's interior, *J. geophys. Res.*, **57,** 227.

Buneman, O., 1969. *A Compact Non-Iterative Poisson Solver*, SUIPR Report, Institute for Plasma Research, Stanford University, Stanford, California.

Busse, F. H. & Schubert, G., 1971. Convection in a fluid with two phases, *J. fluid Mech.*, **46,** 801.

Dufort, E. C. & Frankel, S. P., 1953. Stability conditions in the numerical treatment of parabolic differential equations, *Mathematical Tables and Other Aids to Computation*, **7,** 135.

Isacks, B., Oliver, J. & Sykes, L., 1968. Seismology and the new global tectonics, *J. geophys. Res.*, **73,** 5855.

Schubert, G. & Turcotte, D. L., 1971. Phase changes and mantle convection, *J. geophys. Res.*, **76,** 1424.

Spiegel, E. A. & Veronis, G., 1960. On the Boussinesq approximation for a compressible fluid, *Astrophys. J.*, **131,** 443.